REVISITING THE SCATTERING GREENHOUSE EFFECT OF CO_2 ICE CLOUDS

D. KITZMANN
Center for Space and Habitability, University of Bern, Sidlerstr. 5, 3012 Bern, Switzerland; daniel.kitzmann@csh.unibe.ch

ABSTRACT

Carbon dioxide ice clouds are thought to play an important role for cold terrestrial planets with thick CO_2 dominated atmospheres. Various previous studies showed that a scattering greenhouse effect by carbon dioxide ice clouds could result in a massive warming of the planetary surface. However, all of these studies only employed simplified two-stream radiative transfer schemes to describe the anisotropic scattering. Using accurate radiative transfer models with a general discrete ordinate method, this study revisits this important effect and shows that the positive climatic impact of carbon dioxide clouds was strongly overestimated in the past. The revised scattering greenhouse effect can have important implications for the early Mars, but also for planets like the early Earth or the position of the outer boundary of the habitable zone.

Key words: astrobiology – planets and satellites: atmospheres – radiative transfer

1. INTRODUCTION

Clouds are common in the atmospheres of solar system planets and are likely ubiquitous in those of extrasolar planets as well. They affect every aspect of a planetary atmosphere, from radiative transfer, to atmospheric chemistry and dynamics, and they influence—if not control—aspects such as the surface temperature and, thus, the potential habitability of a terrestrial planet (Marley et al. 2013). Understanding the impact of clouds is thus instrumental for the study of planetary climates.

Clouds composed of carbon dioxide (CO_2) ice particles are important for cold, CO_2-rich atmospheres. This includes, for example, the present and early Mars (Forget & Pierrehumbert 1997), the early Earth (Caldeira & Kasting 1992), or terrestrial exoplanets at the outer boundary of the habitable zone (HZ; Kasting et al. 1993; Forget & Pierrehumbert 1997). Provided that condensation nuclei are available, such clouds would form easily in a supersaturated atmosphere.

Such as in the case of water clouds (e.g., Kitzmann et al. 2010), the presence of CO_2 clouds will first result in an increase of the planetary albedo by scattering incident stellar radiation back to space, which leads to a cooling effect (albedo effect). In contrast to liquid or solid water, CO_2 ice is mostly transparent with respect to absorption in the infrared (Hansen 1997, 2005). Thus, as argued by Forget & Pierrehumbert (1997) or Kasting et al. (1993), a classical greenhouse effect by absorption and re-emission of thermal radiation is unlikely to occur for a cloud composed of dry ice. On the other hand, CO_2 ice particles can efficiently scatter thermal radiation back to the planetary surface, thereby exhibiting a scattering greenhouse effect. In their seminal study, Forget & Pierrehumbert (1997) showed that this scattering greenhouse effect of CO_2 ice clouds alone would have been efficient enough to allow for liquid water on the surface of the early Mars. This strong heating effect was also found in later studies by, e.g., Pierrehumbert & Erlick (1998), Mischna et al. (2000), or Colaprete & Toon (2003). However, by using three-dimensional general circulation models, it has been suggested, that a limiting factor for the impact of CO_2 clouds on early Mars might be the cloud coverage, which could be well below 100% (Forget et al. 2013).

In particular, the outer boundary of the classical HZ might also be influenced by the formation of CO_2 ice clouds and their corresponding climatic impact. For the Sun, Forget & Pierrehumbert (1997) reported an outer HZ boundary of 2.4 AU for a planet fully covered with CO_2 clouds, which is far larger than the cloud-free value of 1.67 AU Kasting et al. (1993).

The competing radiative cooling and heating effects are individually large, but partly balance each other. That means that small errors in the description of one of these radiative interactions can lead to large errors in a cloud's net effect. So far, all previous studies on the climatic impact of CO_2 clouds used a simplified treatment for the numerical solution of the radiative transfer equation to determine the atmospheric and surface temperatures. In particular, two-stream methods (Toon et al. 1989) have exclusively been used. With only two angular directions available to determine the radiation field, these methods provide only limited means to describe e.g., the scattering phase function of the CO_2 ice particles well enough to yield accurate results for describing radiative effects based on anisotropic scattering.

In a numerical radiative transfer study by Kitzmann et al. (2013), it was shown that these simplified two-stream methods underestimate the albedo effect at short wavelengths and overestimate the back-scattering of thermal radiation that forms the basis of the scattering greenhouse effect. However, this previous study did not use an atmospheric model and, thus, was unable to estimate the impact of a more accurate description of the scattering greenhouse effect on the surface temperature.

In this study, I will therefore re-asses the climatic impact of CO_2 clouds using a sophisticated radiative transfer scheme. Since most of the studies related to the climatic impact of CO_2 ice clouds have been done for early Mars, I will use the same modeling scenario to compare my atmospheric model calculations with the previously published results.

2. MODEL DESCRIPTION

To investigate the impact of CO_2 ice clouds, I use a one-dimensional radiative–convective climate model. The model incorporates a state-of-the-art radiative transfer treatment based on a discrete ordinate method (Hamre et al. 2013) which is able
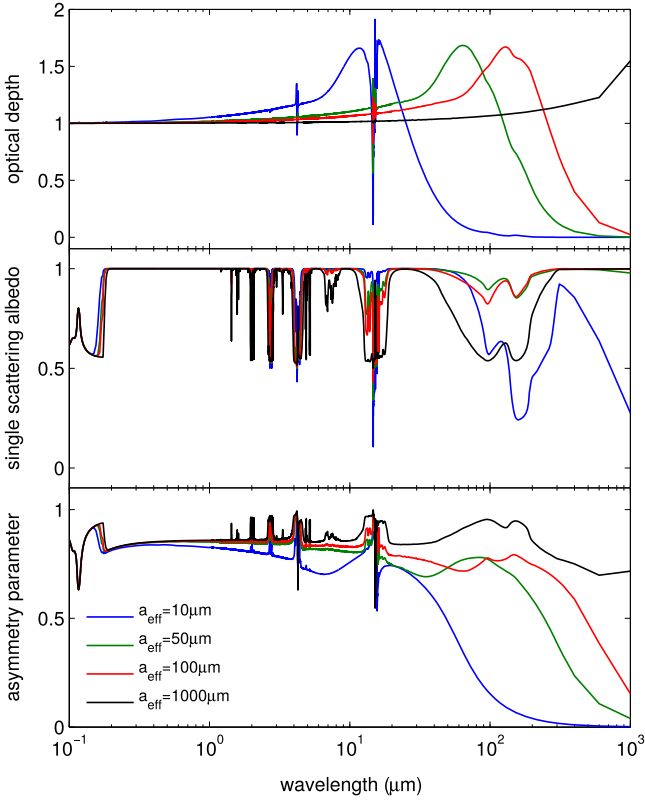
Figure 1. Optical properties of CO_2 ice particles. Results are shown for four different size distributions: $a_{eff} = 10\,\mu m$ (blue line), $a_{eff} = 50\,\mu m$ (green line), $a_{eff} = 100.0\,\mu m$ (red line), and $a_{eff} = 1000\,\mu m$ (black line). Upper diagram: optical depth (for $\tau = 1$), middle diagram: single scattering albedo, lower diagram: asymmetry parameter.

to treat the anisotropic scattering by cloud particles accurately (Kitzmann et al. 2013).

The atmospheric model is stationary, i.e., it does not contain an explicit time dependence, and assumes hydrostatic equilibrium. About one hundred grid points are used to resolve the vertical extension of the atmosphere. The model currently considers N_2, CO_2, and H_2O. Of those, only CO_2 and H_2O are, however, used in this study.

The temperature profile is calculated from the requirement of radiative equilibrium by a time-stepping approach, as well as performing a convective adjustment, if necessary. The convective lapse rate is assumed to be adiabatic, taking into account the condensation of H_2O and CO_2. A surface albedo of 0.215 based on measurements of present Mars is used (Kieffer et al. 1977). A more detailed model description will be presented in D. Kitzmann (2016, in preparation).

2.1. Radiative Transfer

In contrast to many other atmospheric models for terrestrial exoplanets, the radiative transfer of this study is not separated into two different wavelength regimes. Instead, one single, consistent radiative transfer scheme within the wavelength range from 0.1 to 500 μm is used. At each distinct wavelength point, the plane-parallel radiative transfer equation

$$\mu \frac{dI_\lambda}{d\tau_\lambda} = I_\lambda - S_{\lambda,*}(\tau_\lambda) \qquad (1)$$

is solved, with the general source function

$$S_\lambda(\tau_\lambda) = S_{\lambda,*}(\tau_\lambda) + (1 - \omega_\lambda)B_\lambda$$
$$+ \frac{\omega_\lambda}{2} \int_{-1}^{+1} p_\lambda(\mu, \mu')I_\lambda(\mu')d\mu', \qquad (2)$$

where $S_{\lambda,*}$ is the contribution of the central star, B_λ is the Planck function, ω_λ is the single scattering albedo, and $p_\lambda(\mu, \mu')$ is the scattering phase function.

The scattering phase function is represented as an infinite series of Legendre polynomials (Chandrasekhar 1960)

$$p_\lambda(\mu, \mu') = \sum_{n=0}^{\infty} (2n + 1)P_n(\mu)P_n(\mu')\chi_{\lambda,n} \qquad (3)$$

with the Legendre polynomials $P_n(\mu)$ and the phase function moments $\chi_{\lambda,n}$. In practice, the series is truncated at a certain $n = N_{max}$. For discrete ordinate methods, the number of moments N_{max} is equal to the number of ordinates (streams) considered in the radiative transfer equation (Chandrasekhar 1960).

The equation of radiative transfer is solved by the discrete ordinate solver C-DISORT (Hamre et al. 2013). In contrast to two-stream methods, it yields the mathematically exact solution of the transfer equation for a given set of transport coefficients and phase functions, provided that enough computational streams are included. For this study, eight streams are used for all model calculations. Doubling the number of streams has no impact on the resulting radiation fluxes and surface temperatures.

The wavelength-dependent absorption by atmospheric molecules and clouds is treated by the opacity sampling method, which is one of the standard methods employed in cool stellar atmospheres (Sneden et al. 1976). In contrast to the k-distribution method with the correlated-k assumption, opacity sampling still operates in the usual wavelength/wavenumber space (Mihalas 1978). This approach has the advantage, that absorption coefficients of all atmospheric constituents are fully additive. Essentially, opacity sampling can be regarded as a degraded line-by-line formalism. It is based on the fact that the wavelength integral of the radiation flux already converges well before all spectral lines are fully resolved. At each single wavelength, however, the solution with the opacity sampling method is identical to a corresponding line-by-line radiative transfer.

For this study, the distribution of the wavelength points at which the equation of radiative transfer is solved, is treated separately in three different wavelength regions. In the infrared, the points are sampled along the Planck blackbody curves for different temperatures. This method is adopted from Helling & Jorgensen (1998) and guarantees an accurate treatment of the thermal radiation with a small number of wavelength points. In the visible and near-infrared region, 10,000 wavelength points are distributed equidistantly in wavenumbers. This region is most important for the temperature profile in the upper atmosphere where the temperatures are essentially determined by the absorption of stellar radiation within well-separated lines. Beyond the visible wavelength region, about 100 points are used to cover the smooth Rayleigh scattering slope and to resolve the stellar Lyman-α emission line. In total, about 12,500 discrete wavelength points are used here. Tests by increasing the wavelength resolution show virtually no change in the wavelength-integrated flux. In fact, the high number of

integration points in the near-infrared region could also be decreased if one is not interested in the temperatures near the top of the atmosphere.

Absorption cross-sections for CO_2 and H_2O are calculated as described in Wordsworth & Pierrehumbert (2013), using the HITRAN 2012 database (Rothman et al. 2013). For these calculations, the open source *Kspectrum* code (version 1.2.0) is used. In the case of CO_2, the sub-Lorentzian line profiles of Perrin & Hartmann (1989) are employed, while the contribution of collision-induced absorption (CIA) is taken from Baranov et al. (2003). The continuum absorption of H_2O is derived from the MT-CKD description (Mlawer et al. 2012). Rayleigh scattering is considered for CO_2 and H_2O (von Paris et al. 2010).

2.2. Cloud Description

The atmospheric model also takes the radiative effect of clouds directly into account. Following Forget & Pierrehumbert (1997), the size distribution of the CO_2 ice particles is described by a modified gamma distribution

$$f(a) = \frac{(a_{\mathrm{eff}}\nu)^{2-1/\nu}}{\Gamma\left(\dfrac{1-2\nu}{\nu}\right)} a^{(\frac{1}{\nu}-3)} e^{-\frac{a}{a_{\mathrm{eff}}\nu}} \qquad (4)$$

described by the effective radius a_{eff} and an effective variance of 0.1 (Forget & Pierrehumbert 1997).

Assuming spherical particles, the optical properties are calculated via the Mie theory, using the refractive index of CO_2 ice from Hansen (1997, 2005). The resulting optical properties are shown in Figure 1 for some selected values of the effective radius and an optical depth of one. The optical depth, τ, of the clouds refers to the particular wavelength of $\lambda = 0.1\,\mu$m throughout this study.

The Henyey–Greenstein function (Henyey & Greenstein 1941) is used to approximate the scattering phase function. Although it lacks the complicated structure and detailed features of the full Mie phase function, the Henyey–Greenstein function preserves its average quantities, such as the asymmetry parameter g. The Henyey–Greenstein phase function is usually a very good replacement for the Mie phase function, especially at higher optical depths or if one is only interested in angular averaged quantities, such as the radiation flux (van de Hulst 1968; Hansen 1969).

3. EFFECT OF CO_2 CLOUDS IN THE EARLY MARTIAN ATMOSPHERE

To compare the climatic impact of CO_2 ice clouds with previous model studies, I use the same model set-up as in Forget & Pierrehumbert (1997), who studied the influence of CO_2 clouds in the atmosphere of the early Mars.

Thus, following Forget & Pierrehumbert (1997) or Mischna et al. (2000), a CO_2 surface pressure of 2 bar is used on a planet with the radius and mass of Mars. To simulate the conditions for early Mars with a less luminous Sun, the incident stellar flux is set to 75% of the present-day Martian Solar irradiance. A high-resolution spectrum of the present-day Sun from Gueymard (2004) is used for the spectral energy distribution of the incident stellar flux.

Because a supersaturated CO_2-rich atmosphere would provide a huge amount of condensible material, dry ice particles would grow rapidly, thereby potentially reaching large
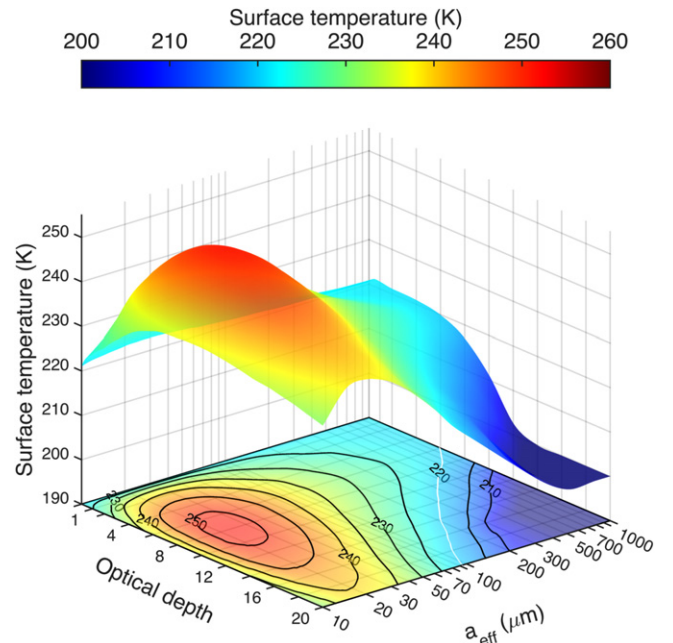

Figure 2. Impact of CO_2 ice clouds on the surface temperature. Surface temperatures are shown as a function of optical depth (at a wavelength of $\lambda = 0.1\,\mu$m) and effective particle size of the CO_2 ice clouds. The black contour lines are given in steps of 5 K. The white contour line indicates the clear-sky case.

particle sizes under these conditions. The only detailed microphysical study for particle formation on early Mars obtained mean particle sizes of the order of 1000 μm (Colaprete & Toon 2003). Thus, to cover this very wide parameter range, the effective particle sizes are varied between 10 and 1000 μm in the following. A total cloud coverage is assumed to obtain an upper limit for the clouds' climatic impact. The cloud layer is placed into the supersaturated region of the cloud-free atmosphere around a pressure of 0.1 bar. This corresponds roughly to the position of the cloud layer in Forget & Pierrehumbert (1997) and Mischna et al. (2000).

Since the publication of Forget & Pierrehumbert (1997) or Mischna et al. (2000), several updates to the molecular line lists and descriptions of the molecule's continuum absorption were introduced. While the greenhouse effect of CO_2 became less effective (Wordsworth et al. 2010), the absorptivity of H_2O increased, especially due to changes in the continuum absorption (Mlawer et al. 2012) and the line parameters (Rothman et al. 2013). Therefore, to limit the impact of the different molecular line lists on the comparison, only CO_2 is considered to be an atmospheric gas in the following. This corresponds to the "dry case" in Forget & Pierrehumbert (1997).

In the clear-sky case, the surface temperature is about 220 K and thus roughly 8 K smaller than reported by Forget & Pierrehumbert (1997) and Mischna et al. (2000). This is caused by a revised CIA of the CO_2 gas, yielding a smaller greenhouse effect (Wordsworth et al. 2010).

The resulting surface temperatures for the cloudy cases are shown in Figure 2 as a function of the cloud particle sizes and optical depth. In total, several hundreds of individual model calculations have been performed to obtain the results in Figure 2.
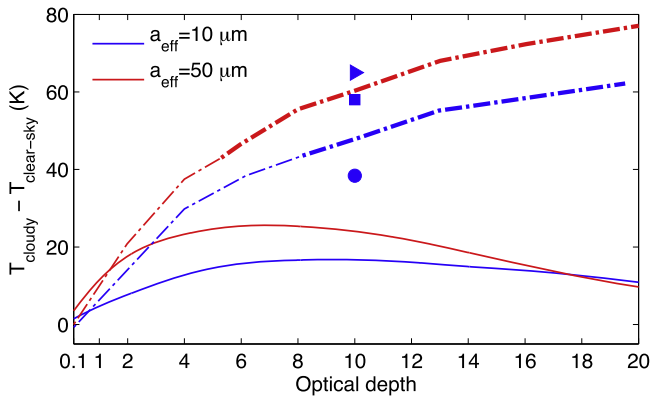
Figure 3. Comparison of the impact of CO_2 clouds on the surface temperature with previous studies. The diagram shows the changes of the surface temperature in the presence of CO_2 ice clouds (T_{cloudy}) with respect to the clear-sky case ($T_{clear-sky}$), compared to the results of Forget & Pierrehumbert (1997) and Mischna et al. (2000). Thicker lines refer to surface temperatures above the freezing point of water. The results are shown for two effective radii: $a_{eff} = 10\ \mu m$ (blue) and $a_{eff} = 50\ \mu m$ (red). Solid lines denote the results from this study, dashed–dotted lines denote the dry atmosphere results from Forget & Pierrehumbert (1997) for comparison. The single three blue markers compare results for an atmosphere fully saturated with water (circle: this study, square: Mischna et al. 2000, triangle: Forget & Pierrehumbert 1997).

In agreement with previous studies (Forget & Pierrehumbert 1997; Pierrehumbert & Erlick 1998; Mischna et al. 2000; Colaprete & Toon 2003), CO_2 particles with effective radii larger than about 10 μm can result in a net greenhouse effect. An efficient greenhouse effect, however, is only possible within a certain particle size range and for medium values of the optical depth. Particles larger than roughly 500 μm are more or less neutral, or—at high optical depths—even exhibit a net cooling effect. These particles are too large to feature an efficient back-scattering of the upwelling thermal radiation. Their large asymmetry parameters at thermal infrared wavelengths result in thermal radiation being predominantly scattered in the upward direction and, thus, away from the surface. In order to obtain the highest possible greenhouse effect, the particle sizes must be comparable to the wavelength of the atmospheric thermal radiation below the cloud layer (see also Kitzmann et al. 2013). This is only the case for $a_{eff} \approx 25\ \mu m$, which therefore provides the largest net greenhouse effect.

In no case studied here is the freezing point of water reached —in contrast to previous studies where surface temperatures in excess of 300 K had been found for the same scenario (Forget & Pierrehumbert 1997). The highest surface temperatures obtained for a pure 2 bar CO_2 atmosphere are about 252 K. Even considering the 8 K difference due to the revised CO_2 CIA, the differences in the resulting surface temperatures between the different radiative transfer approaches are astonishingly large. However, it should be noted, that the lower CIA of the CO_2 molecules might also influence the resulting scattering greenhouse effect of the ice particles to a certain extent.

A direct comparison of the climatic impact with the previous studies of Forget & Pierrehumbert (1997) and Mischna et al. (2000) is shown in Figure 3. Note that Forget & Pierrehumbert (1997) only used two effective radii (10 and 50 μm), while Mischna et al. (2000) are limited to a single value of 10 μm and study only atmospheres saturated with water vapor.
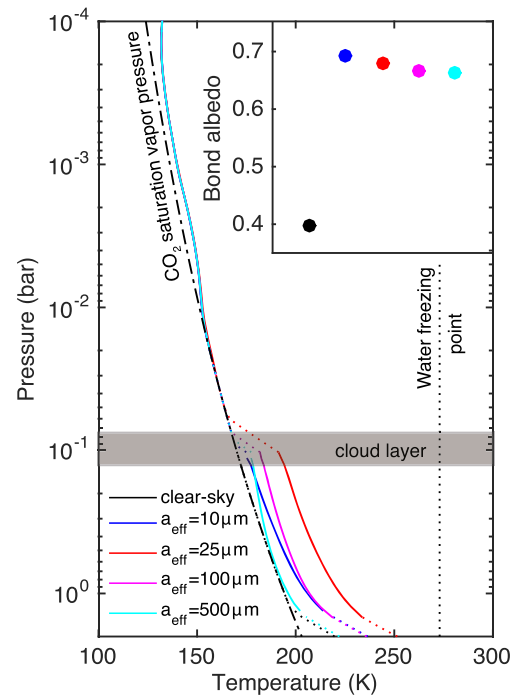

Figure 4. Atmospheric temperature–pressure profiles for the dry case influenced by CO_2 clouds. The resulting temperature profiles are shown for the clear-sky case (black line) and for several values of the effective radius of the particle size distribution (see the legend). The optical depth is 8 in each case. The effect of CO_2 clouds on the energy transport is marked by different line-styles. Solid lines indicate a temperature profile in radiative equilibrium, dashed lines indicate dry convective regions, and the dashed–dotted line indicates a moist CO_2 adiabatic lapse rate. The vertical dotted line denotes the freezing point of water. The dashed–dotted line marks the saturation vapor pressure curve of CO_2. The position of the cloud layer is denoted by the gray-shaded area. The inset plot shows the planetary Bond albedos affected by the presence of the CO_2 ice clouds. Colors refer to the same effective particle sizes mentioned above.

The results in Figure 3 clearly suggest that the climatic impact of CO_2 clouds was strongly overestimated in the past. The cloud-induced temperature changes determined here are several tens of Kelvin smaller in most cases. For an optical depth of 10 and an effective radius of 10 μm, the results for a water-saturated atmosphere are compared. Again, the temperature increases due to the scattering greenhouse effect are between 20 and 30 K smaller than those found in Forget & Pierrehumbert (1997) or Mischna et al. (2000) for this particular case. Additionally, Colaprete & Toon (2003) also claimed a strong greenhouse effect for particle sizes of several hundred μm, which, as already shown in Figure 2, is clearly not the case.

The presence of CO_2 clouds also has a profound impact on the temperature profile, as shown in Figure 4. Due to their scattering greenhouse effect, they strongly increase the atmospheric temperature *locally*, just below the cloud base. This inhibits convection and creates a temperature profile where the usual fully convective troposphere is changed into a lower convective region near the surface and a second one above the cloud layer. Both convective regions are separated by a temperature profile determined by radiative equilibrium (see also Mischna et al. 2000). The local heating due to the cloud particles is in fact strong enough to cause their evaporation. Thus, such a cloud layer would be unable to persist in stationary equilibrium (Colaprete & Toon 2003). Placing the

cloud layer even higher up in the atmosphere would also result in the strong local heating.

Overall, the Bond albedos in the cloudy cases are somewhat higher than the ones reported by previous studies. This is caused by the underestimation of the cloud's albedo effect by the two-stream radiative transfer schemes (Kitzmann et al. 2013).

4. SUMMARY

In this study, the potential impact of the scattering greenhouse effect of CO_2 ice clouds on the surface temperature is revisited by using an atmospheric model with an accurate radiative transfer method. By comparison with previous model studies on the early Mars, the results suggest that the potential heating effect was strongly overestimated in the past.

Based on the results presented here, it is, therefore, strongly recommended that atmospheric models that include the climatic effect of CO_2 ice clouds employ more suitable radiative transfer schemes. Additionally, previous model calculations involving the effect of CO_2 ice clouds, such as for the position of the outer boundary of the HZ or the atmosphere of early Mars, for example, clearly must be revisited. This study also emphasizes the importance of using detailed radiative schemes when studying phenomena based on anisotropic scattering.

While the results for the scattering greenhouse effect found in this study are by far smaller than those reported in previous studies, this does not mean that CO_2 ice clouds are ineffective overall in warming planetary atmospheres. On the contrary, they can still provide an important contribution to the greenhouse effect in a certain parameter range. Thus, the original idea brought up by Forget & Pierrehumbert in their pilot study about a net scattering greenhouse effect still prevails, albeit much smaller than originally anticipated.

REFERENCES

Baranov, Y. I., Lafferty, W. J., Fraser, G. T., & Vigasin, A. A. 2003, JMoSp, 218, 260

Caldeira, K., & Kasting, J. F. 1992, Natur, 359, 226

Chandrasekhar, S. 1960, in Radiative Transfer, ed. S. Chandrasekhar (New York: Dover)

Colaprete, A., & Toon, O. B. 2003, JGRE, 108, 5025

Forget, F., & Pierrehumbert, R. T. 1997, Sci, 278, 1273

Forget, F., Wordsworth, R., Millour, E., et al. 2013, Icar, 222, 81

Gueymard, C. A. 2004, SoEn, 76, 423

Hamre, B., Stamnes, S., Stamnes, K., & Stamnes, J. J. 2013, in AIP Conf. Ser. 1531, International Radiation Symposium (Melville, NY: AIP), 923

Hansen, G. B. 1997, JGR, 102, 21569

Hansen, G. B. 2005, JGRE, 110, E11003

Hansen, J. E. 1969, JAtS, 26, 478

Helling, C., & Jorgensen, U. G. 1998, A&A, 337, 477

Henyey, L. G., & Greenstein, J. L. 1941, ApJ, 93, 70

Kasting, J. F., Whitmire, D. P., & Reynolds, R. T. 1993, Icar, 101, 108

Kieffer, H. H., Martin, T. Z., Peterfreund, A. R., et al. 1977, JGR, 82, 4249

Kitzmann, D., Patzer, A. B. C., & Rauer, H. 2013, A&A, 557, A6

Kitzmann, D., Patzer, A. B. C., von Paris, P., et al. 2010, A&A, 511, A66

Marley, M. S., Ackerman, A. S., Cuzzi, J. N., & Kitzmann, D. 2013, in Comparative Climatology of Terrestrial Planets, ed. S. J. Mackwell et al. (Tucson, AZ: Univ. Arizona Press), 367

Mihalas, D. 1978, Stellar Atmospheres (2nd ed.; San Francisco, CA: W. H. Freeman)

Mischna, M. A., Kasting, J. F., Pavlov, A., & Freedman, R. 2000, Icar, 145, 546

Mlawer, E. J., Payne, V. H., Moncet, J.-L., et al. 2012, RSPTA, 370, 2520

Perrin, M. Y., & Hartmann, J. M. 1989, JQSRT, 42, 311

Pierrehumbert, R. T., & Erlick, C. 1998, JAtS, 55, 1897

Rothman, L. S., Gordon, I. E., Babikov, Y., et al. 2013, JQSRT, 130, 4

Sneden, C., Johnson, H. R., & Krupp, B. M. 1976, ApJ, 204, 281

Toon, O. B., McKay, C. P., Ackerman, T. P., & Santhanam, K. 1989, JGR, 94, 16287

van de Hulst, H. C. 1968, JCoPh, 3, 291

von Paris, P., Gebauer, S., Godolt, M., et al. 2010, A&A, 522, A23

Wordsworth, R., Forget, F., & Eymet, V. 2010, Icar, 210, 992

Wordsworth, R. D., & Pierrehumbert, R. T. 2013, ApJ, 778, 154